Springer

KSME

Journal of Mechanical Science and Technology 25 (8) (2011) 2111~2120
www.springerlink.com/content/1738-494x
DOI 10.1007/s12206-011-0606-6

On the wear mechanism of thin nickel film during AFM-based scratching process using molecular dynamics †

Hanif Muhammad Khan and Sung-Gaun Kim*

Division of Mechanical and Automotive Engineering, Kongju National University, 275 Budae-Dong, Cheonan, 331-717, Korea

(Manuscript Received August 16, 2010; Revised January 10, 2011; Accepted April 6, 2011)

Abstract

We report a study on monocrystalline nickel thin films using the atomic force microscope (AFM) based scratching process to understand the associated wear mechanism. As for the nano level fabrication, better understanding of abrasive wear mechanism is a pre-requisite. A three-dimensional molecular dynamics (MD) study has been performed and we have used a new parameter wear volume to distinguish between different wear zones. A reduced number of zones have been proposed to understand the wear mechanism during nanoscratching process. Also, centrosymmetry parameter has been used to validate the findings.

Keywords: AFM; Molecular dynamics; Nano scratching; NEMS; Nickel; Wear volume

1. Introduction

The atomic force microscope (AFM) has been used to measure mechanical properties of thin films, polymers, and ceramics [1-3]. However, fabrication of nano level system using AFM as a top-down approach would be feasible for simple structures in comparison to the bottom up approach, which is necessary for complex structures. Fabrication of a nanoelectro-mechanical system (NEMS) has been proposed to be fabricated by atomic force microscope (AFM) based nano-scratching process [4]. A novel AFM-based micro/nano machining system has been proposed by Yan et al. [5] which is similar to conventional CNC machine tools. As material property changes with the reduction of its size to nano level, macro level scratching behavior cannot be applied to analyze nano level fabrications. After the first approach to investigate the nanometric scratching process with copper in the late 1980s, several researches have been performed to explore the insight of scratching process in nanocrystalline materials [6-8]. MD simulation has been a reliable technique over the years for its best-suited analyzing ability. Komanduri et al. [9, 10] performed MD simulation of the nanometric scratching of mono crystalline aluminium to study material deformation, scratching forces, chip formation, exit failure. Also, they performed some methodology like effect of tool geometry on single crystal copper to study the scratching processes [11]. Those works help tremendously to understand the nanometric scratching processes. However, small models were adopted in most of the cases in which results might be affected significantly by the boundary conditions. Also, due to the small models, most of the previous models were based on two-dimensional scratching process or quasi-three-dimensional (plane strain) scratching process. In previous reported works the Morse potential is widely used to study the pairwise interaction between metal atoms and to model interatomic force. It is a pair potential considering only two-body interactions, so it cannot properly describe the metallic bonds. Whereas, many body EAM (embedded atom method) potential can describe the phenomenon of metals more precisely, and that is why it has been adopted for this simulation purpose [12]. Nickel substrate has been chosen for the potential application of thin nickel films in magnetic storage devices and NEMS based technologies [13, 14].

For the successful fabrication of nano level structure using AFM, better understanding of abrasive wear mechanism associated with nanomachining process is a pre-requisite. Also, for successful groove fabrication, the cutting mechanism should be correlated as a function with wear behavior of the material. The wear mechanism during nanoscratching process has been separated into four distinct regimes as no-wear regime, adhering regime, ploughing regime and cutting regime [6]. In the no-wear region, atomic lattice is deformed purely elastically [6]. In the adhering regime, surface atoms of the substrate adhere to the tool. In the ploughing regime, the existence of triangular atom cluster has been shown [6]. The cutting region is characterized by chip formation. Also, it has been reported

† This paper was recommended for publication in revised form by Associate Editor In-Ha Sung

* Corresponding author. Tel.: +82415219253, Fax.: +82415559123
E-mail address: kimsg@kongju.ac.kr

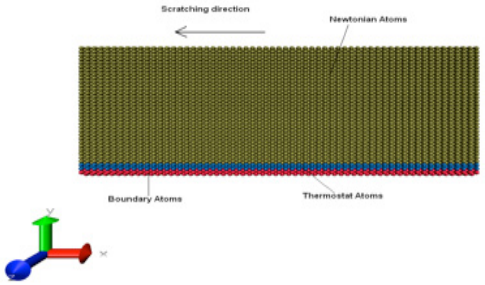

Fig. 1. MD simulation model of nanometric scratching.

that, dislocations distribute closely to the surface or sliding interface [6].

The purpose of the present work is to establish the relation of nanomachining process with the wear mechanism and propose reduced distinct regimes for ease of understanding. This wear mechanism and elastic-plastic transition is closely related, which has been discussed. Previously, evidence of elastic-plastic transition on macro level was reported by Seth [15]. For micro and nano level, evidence of elastic-plastic transition has been reported by Lu et al. [16]. Although it was reported for nanoindentation test, it reveals that there must exist a zone in between.

2. Modeling details

A monocrystalline nickel workpiece has been illustrated on different zones in Fig. 1. The size of the workpiece is 21.12×8.45×16.9 nm and contains 279752 atoms. The lattice constant of nickel is 0.352 nm. The cutting process was along negative x-direction, which is taken as the [-100] direction of the FCC lattice of nickel and on (010) surface. Previously, it has been suggested that the {001} <100> combination should be used for performing simulation of scratching, if only one orientation has to be used, based on nanometric scratching on various scratching directions and crystal orientations [17]. The workpiece consists of three types of atoms: Newtonian atoms, thermostat atoms and boundary atoms. The boundary atoms are kept fixed at their lattice space. Thermostat atoms have been introduced to the system to ensure heat dissipation, which is generated during the scratching process [18]. The temperature of the thermostat atom has been kept at 0 K by rescaling the velocities of the thermostat atoms using velocity rescaling method every hundred computational time, which corresponds to 0.4 ps. Newtonian atoms obey Newton's second law of motion. In molecular dynamics, motions of these atoms are determined by the direct integration of the classical Hamiltonian equations of motion using Velocity-Verlet method [19]. A timestep of 4 fs has been used for the Velocity-Verlet algorithm. Also, periodic boundary condition has been maintained along the z direction. All models were subjected to relaxation for equilibrium state at zero temperature by energy minimization using the conjugate gradient method to allow the models to reach natural and dynamical equilibrium status consistent with the specified temperature.

Fig. 2. Hemi-spherical diamond tool used as tool.

The AFM tool used in this simulation has the shape of a hemi-sphere and is constructed with perfect diamond lattice with a radius of 4.0 nm, shown in Fig. 2. A constant cutting speed of 100 m/s has been used along a cutting distance of 10.0 nm. δ has been varied from 0.1 to 0.5, where δ is a dimensionless parameter which can be defined by d by R ratio. The initial temperature of the workpiece is 0 K. The reasons behind choosing such velocity and temperature are discussed later in this paper.

The force acting on the system is obtained by calculating the forces acting on the atom by the surrounding atoms and encapsulating them. This calculation has been performed using interatomic potentials. The Morse potential is as follows:

$$E_{tot} = \sum_{ij} D_0\{\exp[-2\alpha(r-r_0) - 2\exp[-\alpha(r-r_0)]\} \quad (1)$$

where E_{tot} is a pair potential energy function; D_o is the cohesion energy; α is the elastic modulus; r and r_o are the instantaneous and equilibrium distance between atoms i and j, respectively. Morse potential is a pairwise potential that is not only computationally inexpensive but also simple compared to EAM potential [20].

The EAM method originated from the density-function theory and is based upon the approximation that the cohesive energy of a metal is governed not only by the pairwise potential of the nearest neighbor atoms, but also by embedding energy related to the "electron sea" in which the atoms are embedded. This electron density is approximated by the superposition of atomic electron densities. For EAM potential, the total atomic potential energy of a system is expressed as:

$$E_{tot} = 1/2\sum_{i,j}\phi_{ij}(r_{ij}) + \sum_{i} F_i(\overline{\rho_i}) \quad (2)$$

where ϕ_{ij} is the pair-interaction energy between atoms *i* and *j* and F_i is the embedding energy of atom *i*. ρ_i is the host electron density at site *i* induced by all other atoms in the system, which is given by:

$$\overline{\rho_i} = \sum_{j\neq i}\rho_j(r_{ij}). \quad (3)$$

There are three different atomic interactions in this simulation of nanometric scratching process: the interaction in the workpiece, the interaction between the workpiece atoms and the tool atoms, the interaction in the tool atoms. The EAM potential function for nickel developed by Foiles et al. [21] is used here for the interaction of the substrate atoms. EAM po-

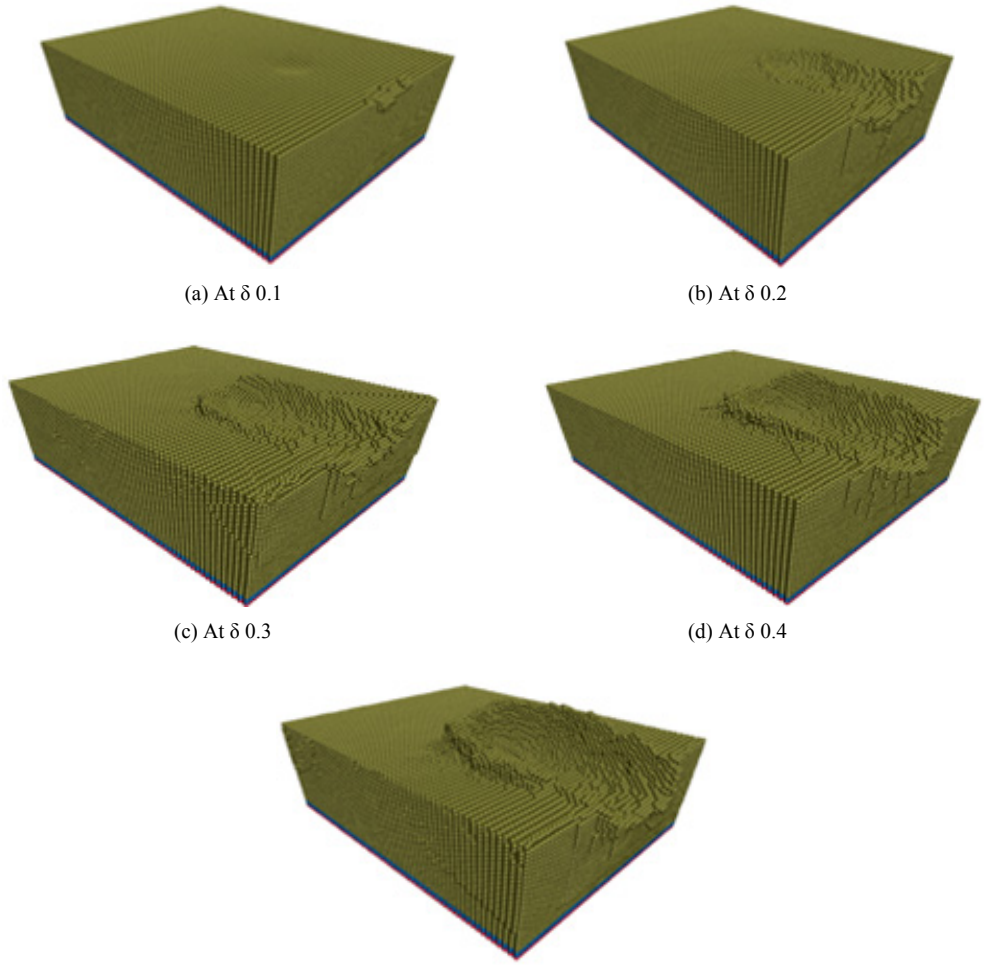

(a) At δ 0.1 (b) At δ 0.2

(c) At δ 0.3 (d) At δ 0.4

(e) At δ 0.5

Fig. 3. Deformation behaviors of scratching process at different dimensionless scratching depths (δ) of 0.1, 0.2, 0.3, 0.4 and 0.5.

tential has been used instead of pairwise Morse potential because the EAM provides a more realistic description of the metallic cohesion, although using Morse potential the energetics of an arbitrary arrangement of atoms can be calculated quickly, but the ambiguity inherited by the volume dependency is avoided by EAM method. For the Ni-C atoms interaction, the Morse potential has been adopted as there is no existing EAM potential available to describe the behavior of interactions between Ni-C atoms. It has been adopted from Fang et al. [22] as D=1.0094 eV, α =0.19875 nm $^{-1}$ and r_0 =2.559 nm. The Lorentz-Berthelot mixing rule was used to estimate the interatomic Morse potential for Ni-C interactions. For the interactions between the tool atoms, also the Morse potential has been adopted where D=2.4230 eV, α=0.25550 nm $^{-1}$ and r_0 =2.522nm. But as the stiffness of a diamond tool is much harder than the stiffness of nickel atoms, the tool can be considered as a rigid body. In this approximation, the interaction force between tool atoms will have no effect on tool atoms. All the simulations of this model use the parallel molecular dynamics program LAMMPS [23-25]. For visualization, an open source molecular visualization program, VMD - visual molecular dynamics, has been used [26].

3. Results and discussion

A three-dimensional model has been used for the current study of AFM-based nanometric scratching process on monocrystalline nickel using an AFM semi-spherical tool. Dimensionless scratching depths of 0.1, 0.2, 0.3, 0.4 and 0.5 have been simulated and their effects on deformation, scratching forces, tribological behavior and wear mechanism have been observed. These parameters could be used effectively to identify elastic-plastic transition, which enables better understanding of abrasive wear mechanism. The discussion provided below is not only from the plots of MD simulations but also from careful observations of the MD simulations.

3.1 On the nature of deformation

Fig. 3 shows the different states of the scratching process during tool travel along the workpiece material with varying scratching depth. The effects have been observed carefully. As

known from solid state physics, as a result of attractive and repulsive forces, metallic atoms are not only arranged in a specific pattern but also they maintain an equilibrium distance in their crystal structures. Conducting a scratching process on a crystallographic material structure will generate a disturbance throughout the metallic structure. The arrangements of the atoms will be changed to create room for the tool to travel along its surface. Hence, deformation occurs. As the tool touches the surface, the crystal structure of the workpiece shows adhesion features with the tool atoms. But with the advancement of the tool on its surface, this adhesion feature no longer exists. Rather, it turns into repulsive nature and the interatomic bonds between workpiece material break due to the advancement of tool atoms. Accumulation of workpiece atoms takes place in front of the tool. It has been found from the simulation that the accumulation not only takes place in front but also beneath the tool edge, and thus a chip is formed. Fig. 4 shows X-Y plane cross sectional view at different stages (with respect to time) of simulation for δ 0.5. Accumulation of substrate atoms and gradual chip formation can be understood from the figure. Also, with the advancement of tool atoms on substrate material surface, atoms pile up on both sides of the tool. As the tool goes forward, these atoms flow towards their respective piling directions to allow the tool to travel. As scratching depth increases, this accumulation and piling up occurs in greater scale. So deformation occurs in large scale. To allow the workpiece to reach a relaxed state, after a certain period, atoms in the workpiece rearrange in crystal structure. Thus, dislocation nucleates and the atoms slip past each other. As the strain energy level on the deformed atoms near to the tool exceeds the limit, the atoms are rearranged on the lower lattice to relax the strain. Due to this rearrangement, a large amount of dislocation takes place. Usually it is generated from the atoms near by the tool and consequently transferred to the whole structure. It has been observed that, the larger is the δ, the more is the dislocation and transformation which takes place around the whole lattice structure. Most of the dislocations glide downwards, and a few glide upwards maintaining some angle. Like the conventional scratching process, fabrication of metal occurs along with chip formation and their removal from the front of the tool. This has been found also in the nanometric scratching process. The dislocations gradually disappear from the crystallographic structure after a certain time period followed by the tool travel for the elastic behavior of the metal [6]. It is evident from the detailed observation that, as the scratching depth increases, the length of adhesion period gets shortened and the repulsion between the tool atoms and the workpiece atoms takes place more rapidly. But as the scratching depth increases, it allows more tool atoms to be in contact with workpiece atoms. So not only the magnitude of the different parameters rises rapidly but also the deformation takes place affecting a greater number of workpiece atoms, indicating the role of greater deformation area. Also, with the increase of scratching depth, roughness of machined surface increases. For lower values of δ, elastic recovery is more favored. In case of 0.1 value of δ, elastic deformation is more dominant than plastic deformation. The transition value lies within 0.1-0.2.

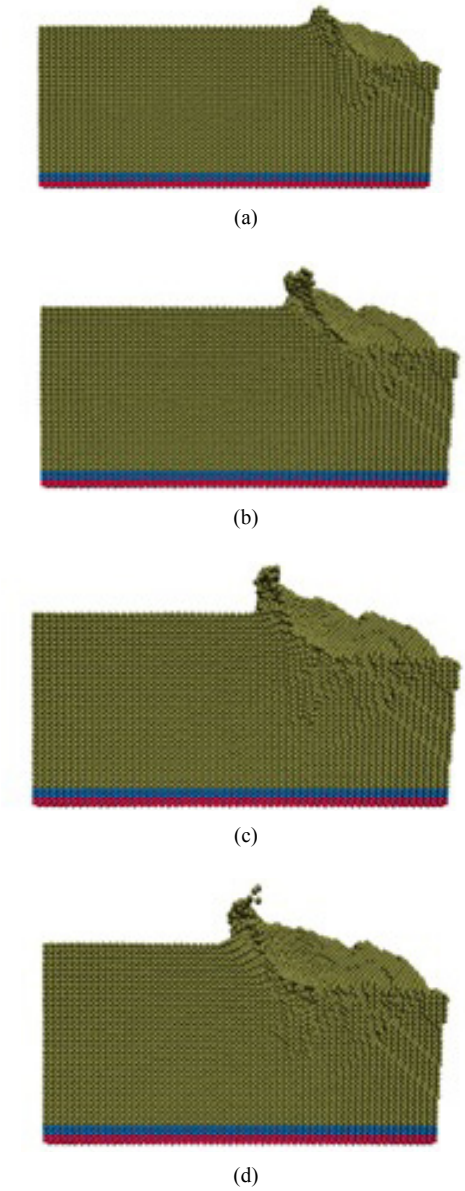

Fig. 4. X-Y plane cross sectional view at different stages of simulation (with respect to time) for δ 0.5: (a) accumulation of substrate atoms; (b), (c) and (d) gradual chip formation.

3.2 On the nature of forces

In the current study, the force in the direction parallel to scratching direction has been considered as the tangential force (x axis) and force in the direction perpendicular to the scratching direction has been considered as the normal force (y axis). The variation of tangential force Fx with scratching distance for the different scratching depth has been plotted in Fig. 5. Usually, less friction and less wear are desirable in

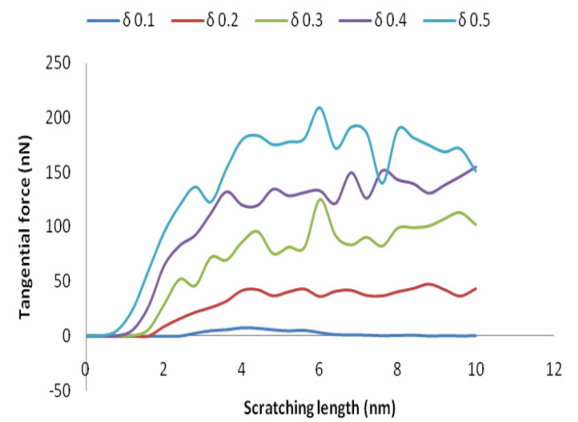

Fig. 5. Variation of tangential forces for five different dimensionless scratching depths (δ) of 0.1, 0.2, 0.3, 0.4 and 0.5.

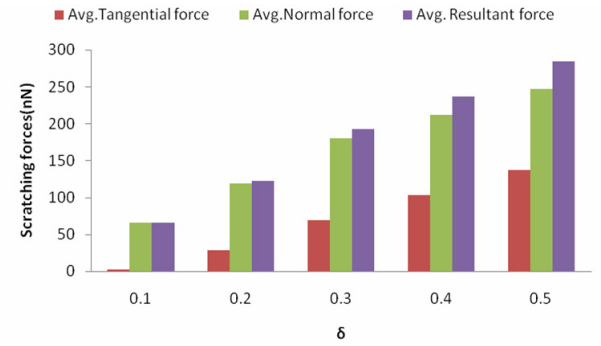

Fig. 6. The time averaged scratching forces for the different dimensionless scratching depths (δ) of 0.1, 0.2, 0.3, 0.4 and 0.5.

practical applications [1]. Both of them are related to adhesion and contact area [1]. Sudden rise in the forces in the initial stage can be explained as follows: if the contact area is high, there exists significant adhesion which gives rise to the tangential force. This adhesion feature determines the elastic or inelastic deformation of the substrate. For small dimensionless scratching depth, like a value of 0.1, there merely exists a sudden rise. Small rise is diminished with gradual elastic recovery of the substrate. On the other hand, for higher dimensionless scratching depths, after the initial sudden rise in tangential force, it reaches to steady state. Although, for different scratching depths, the magnitude is different. The variation is still there in the steady state. More precisely, the variation can be termed as "quasi-periodic variation." After the adhesion, the substrate atoms undergo repulsion and adhesion consecutively with the advancement of the tool. This may be the reason for quasi-periodic variation in the tangential force. Same variation is reported by Buldum and Ciraci [7]. That MD simulation was performed using a sharp Ni tip on a Cu substrate. It can be seen from the MD simulation of the current study that as the δ is less, the fluctuation merely presents like in the case of 0.1 value of δ. With the increase of δ, steady state tends to deviate and presence of rapid fluctuations can be identified. And increased scratching depth requires more

Table 1. MD simulation results for varying δ (dimensionless scratch depth).

δ	Tangential force (nN)	Normal force (nN)	Friction coefficient
0.1	1.9686	66.0919	0.029786
0.2	28.8342	118.6814	0.242955
0.3	68.8343	179.4409	0.383604
0.4	103.5471	211.6488	0.48924
0.5	136.8412	246.8562	0.554336

scratching force for material removal. That can be explained as follows: more material accumulates in front of the tool as scratching depth increases, and the more the scratching force is required for the advancement of the tool and material removal. For lower values of δ, the elastic deformation plays the key role. So, rapid fluctuation in the beginning is absent in that case. On the other hand, higher value of δ induces not only elastic nature but also plastic behavior of materials.

The time-averaged scratching forces have been presented in Fig. 6 with the variation of δ. Although, it has been found that the natures of the plots are similar, only varying in magnitude. Both the tangential force and normal force increase with the increase of dimensionless scratching depth, δ. But the tangential scratching force increases rapidly compared to the normal force. The ratio of normal force to tangential force changes from more than 33 to almost 2. It seems that with increase of δ, contribution of forces is more in tangential force rather than in normal force, as higher scratching force is required for the larger dimensionless scratching depth, δ.

As friction arises from the contact followed by relative movement of two surfaces, it is of obvious need to realize the role of friction in any sort of scratching process. And nevertheless, for a sophisticated process like nanoscratching, it is of immense importance. The values of tangential force and normal force obtained are listed in Table 1. The friction coefficient, which is the ratio of tangential force to normal force, is also provided. The friction coefficient increases with the variation of scratching depth. It can be interpreted that as with the increase of scratching depth, more tangential force is required for tool travel. Because, more material accumulates in front of the scratching tool and requires more external force in scratching direction to remove them, which gives rise to friction coefficient. As friction is the measure of the resistance, this can be utilized to understand the resisting behavior during AFM-based scratching. The friction coefficient has been found to be more dependent on the tangential force than normal force.

3.3 On the wear mechanism

To effectively identify the transition from one regime to another during the nanomachining process, a dimensionless cutting depth δ has been used. This dimensionless cutting depth is the ratio of cutting depth to the tool radius. In this way, the strain induced by the tool on the workpiece will have a rela-

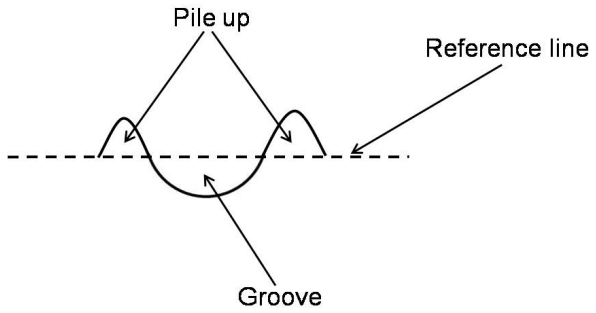

Fig. 7. Schematic of the pile up and groove from the reference line.

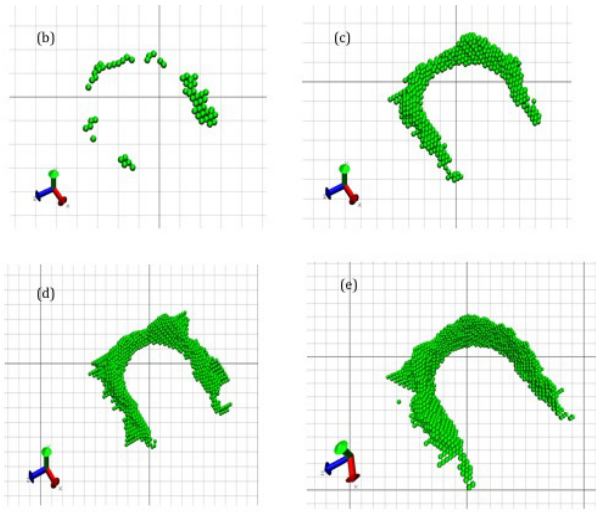

Fig. 8. Pile up pattern during nano machining process for different dimensionless cutting depths (δ) of 0.1, 0.2, 0.3, 0.4 and 0.5. For δ 0.1, it is not shown (a) as there is no pile up. Each grid contains 1 nm^2 area.

tion which would be effective to identify the transition from one regime to other [6]. We have also used pile up volume and the groove volume to understand the associated wear mechanism.

A new parameter, wear volume, has been defined, which is the difference between the groove volume and pile up volume. Schematic of the pile up and groove from the reference line is shown in Fig. 7 where the reference line represents the surface. The proposed reduced model has two regimes: the elastic or no wear regime and the plastic or wear regime. Due to the nature of the scratching process adopted in this work, the groove is shaped like a truncated cylinder with hemispherical end on one side. Simple mathematical equations have been applied for the calculation of groove volume. The patterns of the groove have been carefully observed using VMD to check whether the expected pattern is achieved and mathematical equations hold or not. For the calculation of pile up volume, the pile up pattern is identified above the reference line or surface. The irregularity in the pile up pattern is clearly visible form Fig. 8. It is an alternate close-up representation of Fig. 3 above the reference line that is demonstrated on Fig. 7. The irregular pattern of pile up makes it very difficult to calculate the pile up volume with any well-defined function or equation.

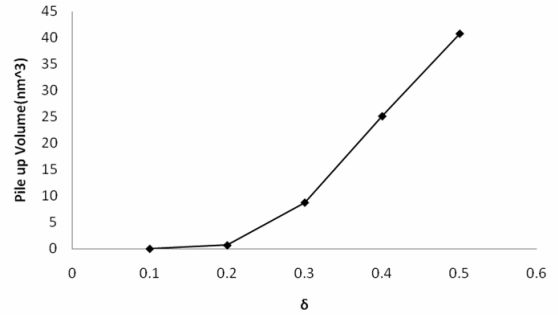

Fig. 9. Variation of Pile up volume at different dimensionless cutting depths (δ) of 0.1, 0.2, 0.3, 0.4 and 0.5.

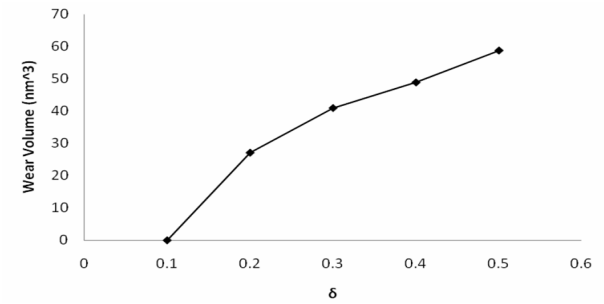

Fig. 10. Variation of Wear volume at different dimensionless cutting depths (δ) of 0.1, 0.2, 0.3, 0.4 and 0.5.

Hence, the number of atoms has been counted on the particular confined region (pile up zone), and volume calculation has been carried out using VMD's scripting procedure. Future work will be focused on putting this pattern in some well-defined function.

Pile up pattern for different values of δ has been illustrated in Fig. 8. Each grid occupies an area of 1 nm^2. For better understanding, only atoms above the reference line have been shown and others have been removed from the visualization. A low value of δ like 0.1 induces no wear on the substrate material. After the machining process, the material recovers almost elastically. Precisely, there is no pile up for such low value of δ. The pile up pattern increases with the increase of δ. The calculated pile up volume has been plotted in Fig. 9. The workpiece material accumulation beyond the reference line after the cutting process has been calculated. To allow the tool to travel through the substrate, workpiece atoms accumulate besides the groove. This also indicates that workpiece atom accumulation not only takes place beneath the tool edge, but also beside the tool edge. On the elastic regime, no groove fabrication is possible due to the elastic recovery of the workpiece material. Calculated wear volume for this zone is almost zero which has been plotted in Fig. 10.

As the value of δ increases from 0.1 to 0.2, nanoscratching process enters in the wear or plastic zone. Pile up pattern is initiated from this region. Also, pile up volume and wear volume increase from their non-zero value. The critical value of transition lies between 0.1 and 0.2 (δ). In this regime, groove fabrication is possible due to plastic deformation and chip

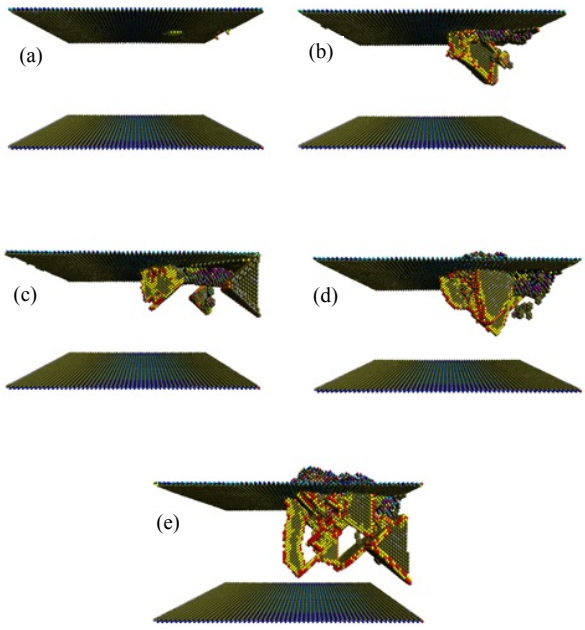

Fig. 11. Defect structure using Centrosymmetry Parameter (CSP) at different dimensionless cutting depths: (a) At δ 0.1; (b) At δ 0.2; (c) At δ 0.3; (d) At δ 0.4; (e) At δ 0.5. Only atoms with CSP>0.5 are shown. In case (a), it is clearly evident that substrate recovers almost elastically after the machining process.

formation. A value greater than zero for pile up indicates the cutting mechanism is in the wear zone and that is also true for the wear volume. In this zone, dislocation takes from the tool edge and glides through the workpiece. The more is the dislocation, the more is the pile up. This enables one to fabricate nano structures using nanoscratching process. Critical value of δ lies between 0.1 and 0.2. Further investigation will be done to identify exactly the transition value.

Finally, the centrosymmetry parameter has been used to identify dislocations and the lattice defects [27]. In solid−state systems the centrosymmetry parameter is a useful measure of the local lattice disorder around an atom and can be used to characterize whether the atom is part of a perfect lattice, a local defect (e.g,. a dislocation or stacking fault), or at a surface. This parameter is computed using the following formula:

$$P = \sum_{i=1}^{6} | \vec{R}i + \vec{R}i+6 |^2 \quad (4)$$

where the 12 nearest neighbors are found and R_i and R_{i+6} are the vectors from the central atom to the opposite pair of nearest neighbors. Atoms not in the group are included in the 12 neighbors used in this calculation. As the material is distorted, these bonds will change direction and/or length, but they will remain equal and opposite under homogeneous elastic deformation. If there is a defect nearby, however, this equal and opposite relation no longer holds. By definition, the centrosymmetry parameter is zero for an atom in a perfect FCC material under any homogeneous elastic deformation, and non-zero for an atom that is near a defect such as a cavity, a dislocation or a free surface.

Dislocations are shown in Fig. 11 using centrosymmetry parameter (CSP). Note that this is the X-Y plane view. Atoms having CSP less than 0.5 have been removed in visualizations. It also satisfies the proposed reduced zones during nanomachining process. During small dimensionless scratching depth, the substrate atoms recover almost elastically, excluding the possibility of groove fabrication. On the other hand, higher dimensionless cutting depth induced machining facilitates the groove fabrication with the aid of plastic deformation. Dislocations glide maintaining an angle of 45 degree with the surface. Glide occurs on generalized {111} planes and in <110> directions. Red colored atoms represent partial dislocations and yellow represent stacking fault.

3.4 Choice of temperature and tool velocity

Improper choice of temperature and velocity might alter the obtained results in the nanoscratching process. When it comes to temperature, an extremely low value (0 K), room temperature (300 K) or elevated temperature (500 K) should be used, but it is still not clear. Again, for tool velocity, whether it should be 1m/s or 500 m/s or in between, the answer is not known precisely. Whatever it might be, still it is much higher than the practically obtainable nanoscratching speed. The subsequent sections address these issues.

The temperature might have a very important role in the estimation of different parameters during nanoscratching process. It influences much of the phase transformation behavior because plastic deformation is a dynamic dissipation process. However, the measures to identify the lattice defects and dislocation such as CNA [28], slip vector [29], and centrosymmetry parameter [27] are sensitive to finite temperature effects [28]. Due to temperature, thermal vibration in atoms exists. Due to this vibration, atoms move from their perfect lattice space and show many partial dislocations [30]. It might significantly affect the dislocation analysis. However, there is no well-defined effect on the tangential scratching force. In Fig. 12, it is shown from previous work [31]. Although, a smaller model has been used for that purpose and the size was 14.1 x 5.6 x 11.3 nm. It contained 83720 atoms. The AFM tool radius was 2 nm. The details can be found from the work. The purpose of thermostating the temperature of thermostat atoms is to couple the system to the surroundings. This is so that the extra amount of heat generated on the substrate could be dissipated to the surroundings like a classical thermodynamic system. If another kind of thermostating procedure is followed, it might alter the phenomenon of a nanoscratching system. Finite temperature imposes fuzzy behavior on dislocation loops [32]. Again, if the system size is too big, damping the thermal vibration of the atoms naturally will take huge amount of time unless some constraints have been imposed such as Nose/Hoover thermostat to total system [33-35]. This might alter the dynamic behavior of the system. For these reasons,

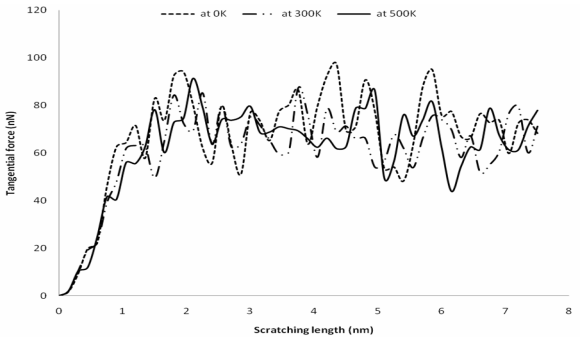

Fig. 12. Variation of tangential force at different temperatures of 0, 300 and 500K [31].

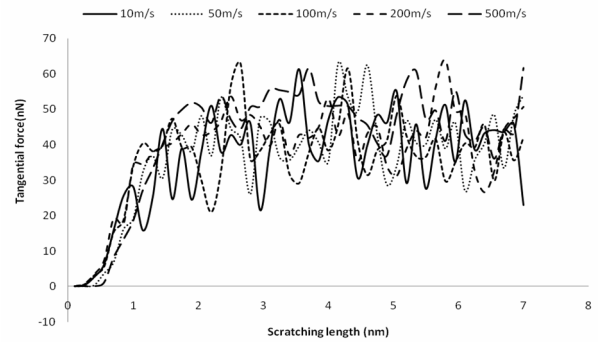

Fig. 13. Variation of tangential force for different scratching velocities [37].

we have chosen an extreme low temperature like 0 K for our work.

If we come to the choice of proper velocity, it is still arguable which one should be used for specific purposes. Although Zhang et al. simulated the scratching velocity dependency during AFM-based scratching process, it is not quite clear which one would be a better choice. Zhang et al. considered the steady state only [36] and found that both average tangential scratching force and friction coefficient increase. They found a decreasing relation with normal force. Pei et al. found increasing relationship for tangential force with tool velocity [30]. However, they found also an increasing relationship for normal force with tool velocity. To find a proper choice we conducted a similar investigation [37]. Tool velocity has been varied from a low value of 10 m/s to a high value of 500 m/s at different intervals on a monocrystalline nickel workpiece containing 35258 atoms. The size of the workpiece was 10.56 x 2 x 5 nm. Tool radius was 2 nm and scratching depth was 1 nm. Variation of tangential force for different scratching velocities is shown in Fig. 13 [37]. It is quite difficult to relate tangential force to tool velocity if unsteady state is taken into consideration in Fig. 13 [37]. We considered the unsteady state along with steady state during averaging, as both are part of the dynamic process. Excluding one might lead to an erroneous conclusion. Surprisingly, we found increase in both average tangential and normal forces except at 100 m/s, shown in Fig. 14 [37]. There is a small amount of drop in friction coefficient up to 100 m/s and then it increases again up to 500 m/s, as shown in Fig. 15 [37]. We also observed a temperature rise of the Newtonian atoms, which is similar to the previous work [36]. It has been plotted on Fig. 16 [37]. The temperature evolution as a function of δ is also provided in Fig. 17. The greater is the δ, the greater is the contact area between the substrate and the tool. Hence, the more is the strain imposed by the tool on the substrate. On the other hand, higher tool velocity also imposes higher strain. Higher strain causes the subsurface deformed atoms to move from their perfect lattice configuration, thus consequently allows plastic deformation of the substrate. The comparison of temperature evaluation of the system with both tool velocity and δ shows the strain induced by the tool velocity is more in comparison

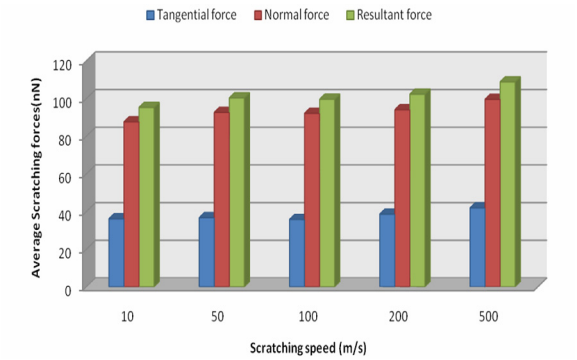

Fig. 14. The time averaged scratching forces for different scratching velocities of 10, 50, 100, 200 and 500 m/s [37].

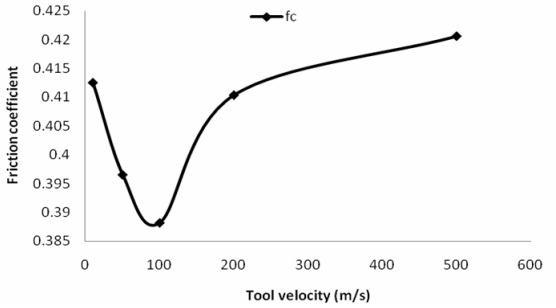

Fig. 15. Variation of friction coefficient with tool velocity [37].

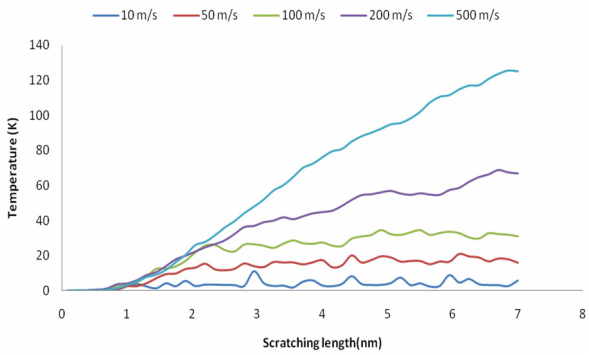

Fig. 16. Variation of temperature of Newtonian atoms for different scratching velocities [37].

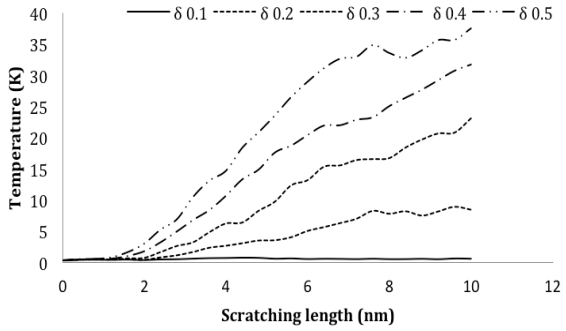

Fig. 17. Variation of temperature of Newtonian atoms for different dimensionless cutting depths (δ).

to the contact area. As temperature at atomic level is related to the kinetic energy of the system, with higher scratching speed of the tool the substrate atoms have to move faster to allow the scratching process. Thus, the temperature of the system rises rapidly with high tool speed. So, the strain imposed by the tool is more dependent on the tool velocity rather than the contact area between the tool and the substrate. Further investigations should be carried out to optimize these parameters.

4. Conclusions

We present an investigation of the wear mechanism of thin nickel films using three-dimensional MD simulations:

(1) A new parameter, wear volume (based on pile up and groove volume), has been proposed to identify transitions from one regime to another. Also, a reduced number of zones have been proposed to understand easily the associated abrasive wear mechanism. This study helps to understand whether groove fabrication is possible or not with the aid of plastic deformation.

(2) Future work will be focused on parameterizing the elastic-plastic transition during nanoscratching process.

(3) Strain energy imposed by the tool on the substrate is more dependent on tool velocity rather than the contact area between tool and the substrate.

Acknowledgment

The authors gratefully acknowledge financial support by Brain Korea 21.

References

[1] B. Bhushan, J. N. Israelachchvii and U. Lundman, Nanotribology: friction, wear and lubrication at the atomic scale, *Nature,* 374 (1995) 607-616.

[2] T. H. Fang, W. J. Chang and S. L. Tsai, Nanomechanical characterization of polymer using atomic force microscopy and nanoindentation, *Microelectronics Journal,* 36 (2005) 55-59.

[3] T. H. Fang and W. J. Chang, Nanomechanical properties of copper thin films on different substrates using the nanoindentation technique, *Microelectronics Engineering,* 65 (2003) 55-59.

[4] L. L. Sohn and R. L. Willett, Fabrication of nanostructures using atomic-force-microscope-based lithography, *Appl. Phys. Lett.,* 67 (1995) 1552-1554.

[5] Y. Yan, T. Sun, Y. Liang and S. Dong, Investigation on AFM-based micro/nano-CNC machining system, *International Journal of Machine Tools & Manufacture,* 47 (2007) 1651-1659.

[6] L. Zhang and H. Tanaka, Towards a deeper understanding of wear and friction on the atomic scale - a molecular dynamics analysis, *Wear,* 211 (1997) 44-53.

[7] A. Buldum and S. Ciraci, Contact, nanoindentation, and sliding friction, *Phys. Rev. B,* 57 (1998) 2468-2476.

[8] K. Maekawa and A. Itoh, Friction and tool wear in nano-scale scratching- a molecular dynamics approach, *Wear,* 188 (1995) 115-122.

[9] R. Komanduri, N. Chandrasekaran and L. M. Raff, Molecular dynamics simulation of atomic scale friction, *Phys. Rev. B,* 61 (2000) 14007-14019.

[10] R. Komanduri, N. Chandrasekaran and L. M. Raff, Orientation effects in nanometric scratching of single crystal materials: an md simulation approach, *Ann. CIRP,* 48 (1999) 67-72.

[11] R. Komanduri, N. Chandrasekaran and L. M. Raff, Effect of tool geometry in nanometric scratching: a molecular dynamics approach, *Wear,* 219 (1998) 84-97.

[12] M. S. Daw and M. I. Baskes, Embedded-atom method: Derivation and application to impurities, surfaces, and other defects in metals, *Phys. Rev. B,* 29 (1984) 6443-6453.

[13] S. D. Leith and D. T. Schwartz, High-rate through-mold electrodeposition of thick (>200m) NiFe MEMS components with uniform composition, *Journal of Microelectromechanical Systems,* 8 (1999) 384-392.

[14] J. K. Luo, A. J. Flewitt, S. M. Spearing, N. A. Fleck and W. I. Milne, Young's modulus of electroplated Ni thin film for MEMS applications, *Materials Letters,* 58 (2004) 2306-2309.

[15] B. R. Seth, Transition theory of elastic-plastic deformation, creep and relaxation, *Nature,* 195 (1962) 896-897.

[16] C. Lu, Y.-W. Mai, P. L. Tam and Y. G. Shen, Nanoindentation-induced elastic-plastic transition and size effect in **α**-Al_2O_3(0001), *Philosophical Magazine Letters,* 87 (2007) 409-415.

[17] R. Komanduri, N. Chandrasekaran and L. M. Raff, MD Simulation of nanometric scratching of single crystal aluminium-effect of crystal orientation and direction of scratching, *Wear,* 242 (2000) 409-415.

[18] W. C. D. Cheong, L. Zhang, and H. Tanaka, Some essentials of simulating nano-surfacing processes using the molecular dynamics method, *Key Engg. Mater. Vols.,* 196 (2001) 31-42.

[19] L. Verlet, Computer "experiments" on classical fluids.I. thermodynamical properties of lennard-jones molecules, *Phys. Rev.,* 159 (1967) 98-103.

[20] Q. X. Pei, C. Lu, F. Z. Fang and H. Wu, Nanometric

scratching of copper: A molecular dynamics study, *Comput. Mater.Sci.,* 37 (2006) 434-441.
[21] S. M. Foiles, M. I. Baskes and M. S. Daw, Embedded-atom-method for the fcc metals Cu, Ag, Au, Ni, Pd, Pt, and their alloys, *Phys. Rev. B,* 33 (1986) 7983-7991.
[22] T. H. Fang and J. H. Wu, Molecular dynamics simulations on nanoindentation mechanisms of multilayered films, *Comput. Mater. Sci.,* 43 (2008) 785-790.
[23] Information of LAMMPS molecular dynamics simulator at http://lammps.sandia.gov/.
[24] S. J. Plimpton and B. A. Hendrickson, Parallel molecular dynamics with the embedded atom method, In: Broughton J, Bristowe P, Newsam J, (editors). Mater. Theory and Modelling, *MRS Proceedings,* 291 (1993) 37.
[25] S. Plimpton, Fast parallel algorithms for short-range molecular dynamics, *J. Comput. Phys.,* 117 (1995) 1-19.
[26] W. Humphrey, A. Dalke and K. Schulten, VMD: Visual molecular dynamics, *J. Mol. Graph.,* 14 (1996) 33-38.
[27] C. L. Kelchner, S. J. Plimpton and J. C. Hamilton, Dislocation nucleation and defect structure during surface indentation, *Phys. Rev. B,* 58 (1998) 11085-11088.
[28] J. Li, K. J. Van Vliet, T. Zhu, S. Yip and S. Suresh, Atomistic mechanisms governing elastic limit and incipient plasticity in crystals, *Nature,* 418 (2002) 307-310.
[29] J. A. Zimmerman, C. L. Kelchner, P. A. Klein, J. C. Hamilton and S. M. Foiles, Surface step effects on nanoindentation, *Phys. Rev. Lett.,* 87 (2001) 1655071-1655074.
[30] Q. X. Pei, C. Lu and H. P. Lee, Large scale molecular dynamics study of nanometric machining of copper, *Comp. Mat. Sci.,* 41 (2007) 177-185.
[31] H. M. Khan and S. G. Kim, Atomistic modeling of scratching process based on atomic force microscope: effects of temperature, *Proc. of 3rd International Nano Electronics Conference*, Hong Kong (2010) 134-135.
[32] D. Sarev and R. E. Miller, Atomic-scale simulations of nanoindentation-induced plasticity in copper crystals with nanometer-sized nickel coatings, *Acta Materialia,* 54 (2006) 33-45.
[33] S. Melchionna, G. Ciccotti and B. L. Holian, Hoover NPT dynamics for systems varying in shape and size, *Molecular Physics,* 78 (1993) 533-544.
[34] S. Nose, A unified formulation of the constant temperature molecular dynamics methods, *J. Chem. Phys.,* 81 (1984) 511-519.
[35] W. G. Hoover, Canonical dynamics: Equilibrium phase-space distributions, *Phys. Rev. A,* 31 (1985) 1695-1697.
[36] J. Zhang, T. Sun, Y. Yan and Y. Liang, Molecular dynamics study of scratching velocity dependency in AFM-based nanometric scratching process, *Mat. Sci. and Engg. A,* 505 (2009) 65-69.
[37] H. M. Khan and S. G. Kim, Effect of tool velocity during AFM-based scratching process: A molecular dynamics approach, *Proc. of International Conference on Nano Science and Nano Technology*, Muan, Korea (2009) 21.

Hanif Muhammad Khan received his B.Sc. in Mechanical engineering from Islamic University of Technology (IUT), Bangladesh in 2008. He received his M.Sc. in Mechanical Engineering from Kongju National University in South Korea. Now he is at the University of Perugia, Italy, studying European Master in Theoretical Chemistry and Computational Modelling (EMTCCM). His research interests include nano-mechanics.

Sung-Gaun Kim is currently working as a Professor in the Department of Mechanical and Automotive Engineering at Kongju National University, Korea. He received his Ph.D. in Mechatronics from Gwangju Institute of Science and Technology and M.S. in Automation and Design Engineering from KAIST (Korea Advanced Institute of Science and Technology), Korea. His current research interests include Molecular Dynamics & Mechanics, Intelligent Robot, Control and Design of bio/nano mechatronics system, Computer Vision, etc. He has published many research papers in various national and international journals and conferences.